Ultrawideband-Based 3-D Localization Using Compact Base-Station Configurations

Richa Bharadwaj, *Student Member, IEEE*, Clive Parini, *Member, IEEE*, and Akram Alomainy, *Senior Member, IEEE*

***Abstract*—This letter presents theoretical and experimental investigations and analysis on three-dimensional ultrawideband (UWB) localization using compact base-station configurations. A comparative study is performed between the three proposed configurations (Y-shape, L-shape, and mirror-based) and the commonly used cuboid-shape configuration in terms of accuracy and compactness. Results show that the average localization accuracy of the Y- and L-shape configurations is in the range of 3–5 cm, whereas the cuboid- and mirror-based configurations give an accuracy of around 2–5 cm. The Geometric Dilution of Precision (GDOP) values have been calculated for all configurations, which shows a high level of accuracy (i.e., precision values are in the range of 2–4). In addition, a tradeoff regarding occupancy area and complexity is taken into account, and the results show that the proposed configurations have the advantage of compactness as compared to the cuboid configuration and also provide high accuracy in centimeter range, hence making it suitable for various applications such as motion capture in healthcare systems and entertainment.**

***Index Terms*—3-D localization, ultrawideband (UWB), time of arrival.**

I. Introduction

ULTRAWIDEBAND (UWB) technology has become one of the major developments in the wireless industry with potential for high-data-rate communication and high-precision time-of-arrival (TOA)-based ranging. UWB technology offers potential applications in high-resolution positioning and ranging in various fields of medical, military, office, and indoor environments [1].

Commercial UWB localization systems such as Ubisense, Multispectral Solutions, Inc., have accuracy of 10–15 cm with operating ranges of greater than 50 m [2]. Higher accuracy in centimeter range (1–5 cm) has been reported in the literature for indoor UWB positioning systems [2]–[4]. An accuracy of centimeter range is being achieved using impulse-based UWB systems, and subcentimeter range accuracy is possible using carrier-based UWB systems as proposed in literature [2]. Related research activities reported in the open literature are based on 3-D localization using a minimum of four base stations (BSs) or more for localizing an object [2]–[5]. It is observed that different configurations and numbers of base stations used have an effect on the accuracy obtained in positioning [2], [5], [6]. In this letter, the main focus is on 3-D localization that is achieved by using compact configurations (by reducing the number of base stations/space occupied) in comparison to conventional methods and those available in the open literature. In addition, Geometric Dilution of Precision (GDOP) is used to theoretically analyze the precision of the base-station configurations.

Three methods are proposed for localization, namely the Y-shape configuration, L-shape configuration, and mirror-based technique. The above three methods reduce the number of base stations/space required for obtaining accurate localization in 3-D and relax the requirement on the amount of area and complexity for setting up the system. Cartesian and directional information are obtained for the proposed models, giving good accuracy in centimeter range. Thus, in the present study, efforts have been made to reduce the complexity, space, and cost of the base-station configurations to achieve high-accuracy 3-D localization. The rest of the letter is organized in different sections dealing with measurement setup, description of the configurations, localization techniques and algorithms, experimental results, theoretical analysis, and the conclusion.

II. Experimental Setup

A compact and low-cost tapered slot (TSA) UWB antenna is used as transmitter and receiver [7]. The TSA antenna has excellent impedance matching with return loss below -10 dB and radiation performance in the UWB range with approximately constant gain over the whole frequency band. The total antenna size is 27×16 mm^2.

The TSA antenna exhibits near-omnidirectional behavior across the higher band of the UWB spectrum except for slight degradation in the lower band due to its compact size and, overall, shows good performance in comparison to other compact designs in the open literature [7].

UWB 3-D localization measurements (Fig. 1) were performed in the 3–10-GHz range in the Body-Centric Wireless Sensor Lab (BCWS) at Queen Mary, University of London, London, U.K. [7]. The TSA antennas were connected to the four-port programmable vector network analyzer (Agilent, PNA-X, N5244A [8]) by low-loss coaxial cables to measure the transmission response (S_{21}). Three BS antennas and one mobile-station (MS) antenna were connected at a time in which the BS acts like the receiver and the MS as the transmitter. The PNA is set to 6400 data samples, which are sufficient to capture all the necessary impulse response information required to provide appropriate statistical data set. The base stations are

Manuscript received December 20, 2013; accepted January 14, 2014. Date of publication January 20, 2014; date of current version February 11, 2014. This work was supported in part by the Queen Mary University of London Principle's Doctoral Scholarship and Engineering and Physical Sciences Research Council (EPSRC), U.K.

The authors are with the School of Electronic Engineering and Computer Science, Queen Mary University of London, London E1 4NS, U.K. (e-mail: r.bharadwaj@qmul.ac.uk; c.g.parini@qmul.ac.uk; a.alomainy@qmul.ac.uk).

Color versions of one or more of the figures in this letter are available online at http://ieeexplore.ieee.org.

Digital Object Identifier 10.1109/LAWP.2014.2301636

1536-1225 © 2014 IEEE. Personal use is permitted, but republication/redistribution requires IEEE permission.
See http://www.ieee.org/publications_standards/publications/rights/index.html for more information.

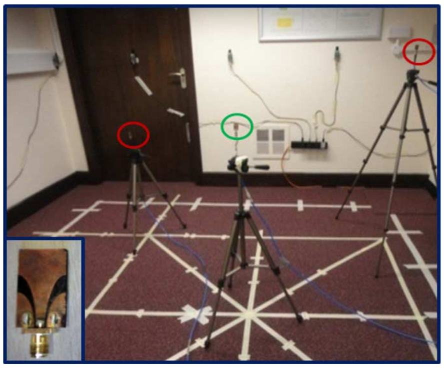

Fig. 1. Measurement setup used for localization of the mobile station that is moved at 17 different positions in an area of 1.5×1.5 m^2. The base stations (red circles) and mobile station (green circle) are connected to the four-port vector network analyzer (PNA-X, N5244A). The tapered slot UWB antenna is shown in the inset.

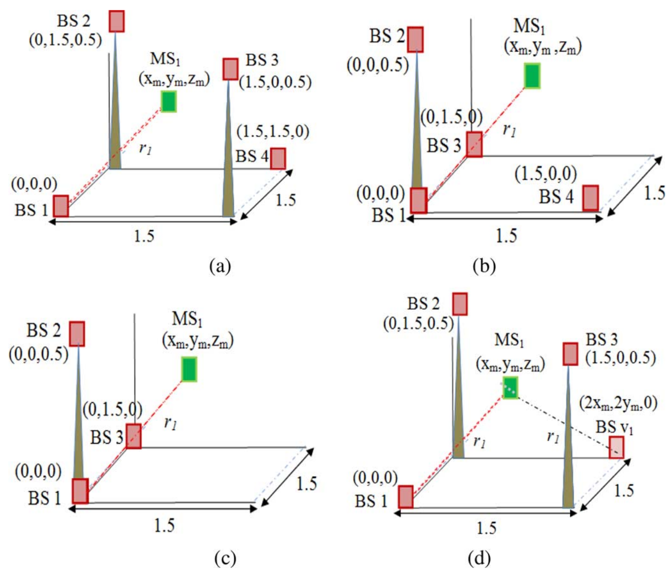

Fig. 2. Configuration of the base-station models (a) cuboid, (b) Y-shape, (c) L-shape, and (d) mirror-based with Base Station 1 at origin (0, 0, 0). The target antenna (mobile station) whose coordinates have to be estimated is placed in the center of the cuboid. All dimensions are in meters.

positioned near the vertices of the cuboid as shown in Fig. 2 to obtain high-accuracy positioning in three dimensions. The antenna at BS1 is considered as reference zero coordinate (x_0, y_0, z_0), which acts as the reference to find the position of the target placed inside the volume of the cuboid. The MS is moved in 17 different positions, with position A at the center of the area (sized 1.5×1.5 m^2) and the rest of the positions at 25 and 50 cm away from the center position. Cartesian coordinates and directional information related to the position of the target are obtained through time-of-arrival data fusion and first peak detection algorithms [9]–[11]. The directional parameters (Fig. 3) of the mobile station are estimated through conversion of Cartesian to spherical coordinates.

III. Base-Station Configurations

In this letter, four different BS configurations are used, which are described briefly in the following.

1) Cuboid-Shape Configuration: The cuboid-shape configuration is shown in Fig. 2(a). Four base stations are used to

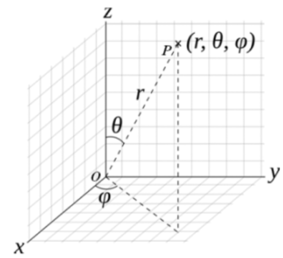

Fig. 3. Spherical coordinate system with origin O, zenith angle θ, and azimuth angle φ.

estimate the location of the unknown target. This configuration is most commonly used for localization as given in literature [2], [6]. Eight base stations can also be used to get more accurate results, but it would make the localization system more complex to install and more expensive.

2) Y-Shape Configuration: The Y-shape configuration is shown in Fig. 2(b). The four base stations are arranged in shape of the letter Y. The distance between the base stations can be adjusted according to the area under observation and for obtaining precise measurement. The proposed configuration occupies less space and gives accurate results that are comparable to the conventional cuboid-shape base-station configuration.

3) L-Shape Configuration: The L-shape model [Fig. 2(c)] uses only three base stations to achieve 3-D localization. First, x- and z-coordinate information is obtained using TOA data fusion method as explained in [10]. The following trigonometric equations are used to find the y-coordinate:

$$\theta = \cos^{-1} \frac{z_m}{R\_\mathrm{est}} \tag{1}$$

$$S = \frac{z_m}{\tan(90 - \theta)} \tag{2}$$

$$y_m = \sqrt{S^2 - x_m^2} \tag{3}$$

where $R_$est is the estimated distance from the BS1 (origin) to the target P. z_m and x_m are the estimated position through TOA data fusion method. θ is the zenith angle, and S is the projected distance of point P from origin in the xy-plane.

4) Mirror-Based Configuration: The Mirror Base Station model is shown in Fig. 2(d). There are three BSs present with known positions, and the fourth base station is the mirror image of BS1 with respect to the position of the MS. In the mirror-based configuration, first 2-D localization is achieved in the xy-plane using three BSs through TOA data fusion technique. In order to obtain the position of BS4, the values of estimated x and y of the MS are doubled, and the height of BS4 is kept the same as BS1. Hence, the coordinates of the new BS4 are $(2x, 2y, 0)$. The range value from BS4 to MS is the same as that of BS1 to MS [the channel impulse response (CIR) is considered same as that of BS1] as BS4 is considered the mirror image of BS1 and, hence, is a virtual base station. Now there are four base stations in total of which ranging values and positions are known. Three-dimensional localization is obtained using TOA data fusion technique [10].

IV. Localization Technique

The accuracy in prediction of TOA is the most important parameter for positioning systems. Channel impulse response and

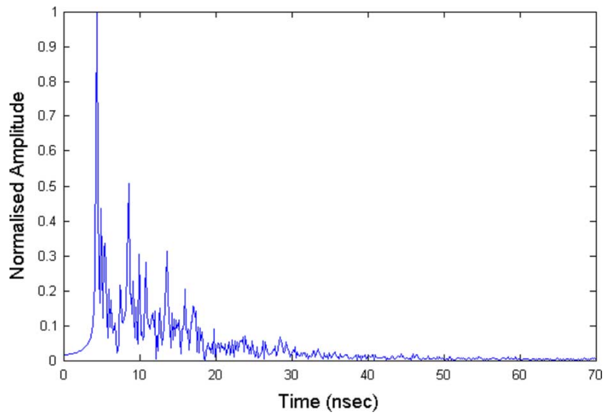

Fig. 4. Channel impulse response in the indoor environment between mobile station and Base Station 1.

peak detection algorithms are used to get accurate TOA/range values between base stations and the mobile station. The transmission coefficient (S_{21}) responses between transmitter and each receiver are measured using the programmable vector analyzer in the BCWS lab. An inverse fast Fourier transform (IFFT) is then applied to obtain the impulse response from the measured channel response (S_{21}). For N propagation paths between the transmitter and the receiver (with the amplitude, phase, and delay of the kth path being α_k, φ_k, and τ_k, respectively), the channel impulse response (Fig. 4) is given by [11], [12]

$$y(t) = \sum_{k=1}^{N} \alpha_k e^{j\varphi_k} \delta(t - \tau_k). \tag{4}$$

The TOA is then determined through peak detection algorithm in which the dominant peak of the CIR will give an estimate of the TOA for the line-of-sight (LOS) case [12]. However, in urban or indoor environments, the accuracy in estimation of TOA depends on the multipath components, non-line-of-sight (NLOS) situations, low signal-to-noise ratios (SNRs), sampling precision of the analyzer, and the environment in which measurements are taking place. Due to the large bandwidth of a UWB signal, multipath components are usually resolvable, but can be challenging in dense multipath environments where the nondominant direct path estimate corresponds to the TOA. A prior knowledge of the environment can help in resolving NLOS and multipath situations. Threshold-based methods such as the leading edge detection and search back method are given in the literature [9]–[11] to detect the first arriving path. The leading edge detection method sets the threshold based on noise level. The search-back method first finds the strongest path (SP), and then looks for a peak arriving before the strongest path that has greater power than a detection threshold level.

The TOA data fusion method [10] is used to find the unknown coordinates of the MS, which is based on combining estimates of the sensor signal TOA that arrive at four different base stations. The distance between each MS and BSi is found by multiplying the TOA estimate with the speed of light. Let r_1, r_2, r_3, and r_4 represent the range measurements obtained from TOA measurements. The following four equations are solved jointly by using least-square solution in order to estimate the position of the target (x_m, y_m, z_m) via trilateration:

$$r_i^2 = (x_i - x_m)^2 + (y_i - y_m)^2 + (z_i - z_m)^2 \qquad i = 1, 2, 3, 4. \tag{5}$$

TABLE I
AVERAGE LOCALIZATION ERROR

Configurations	X axis Error (cm)	Y axis Error (cm)	Z axis Error (cm)
Cuboid Shape	2.1	3.12	3.49
Y Shape	2.35	2.95	5
L Shape	1.81	4.16	5.1
Mirror BS	2.19	2.18	4.8

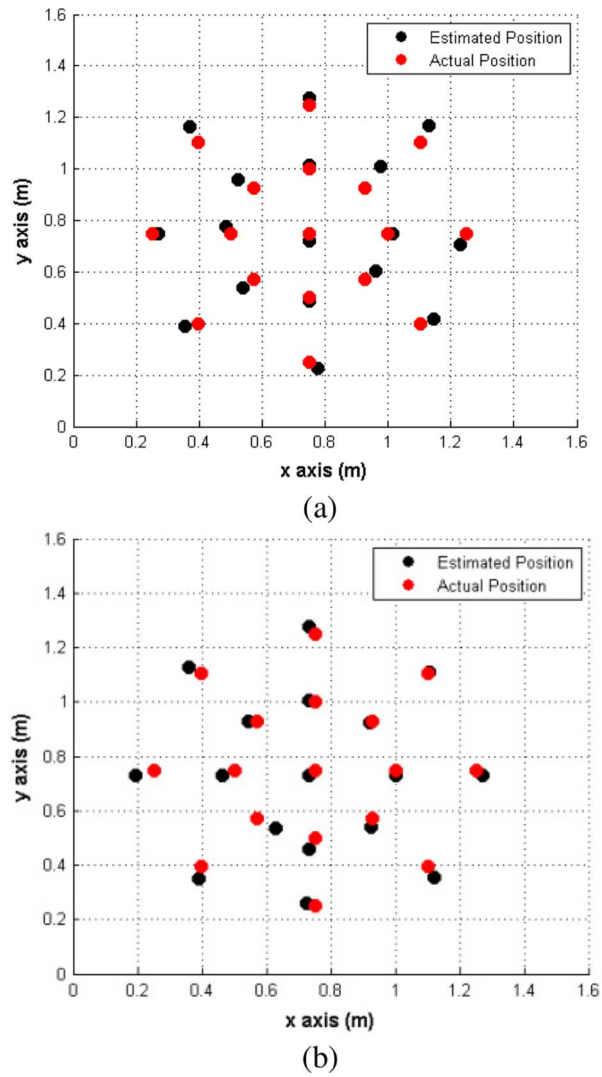

Fig. 5. Comparison of actual (red) and estimated (black) positions of mobile station for (a) Y-shape and (b) mirror-based BS configurations.

V. Localization Accuracy Analysis

Table I. shows the (x, y, z) axis average error for the 3-D experiments for the four BS configurations. For cuboid-shape configuration, the x-axis has smaller average error (2 cm) in comparison to y- and z-axes that have an average error of 3–3.5 cm. The average error obtained for Y-shape configuration [Fig. 5(a)] is in the range of 2–3 cm for x- and y-axes and 5 cm for z-axis. The L-shape configuration shows an average error of 2, 4, and 5 cm for x-, y-, and z-axis, respectively. The y-axis error is higher for L-shape configuration as it is using only three base stations for compact configuration, and it is a good tradeoff between the number of BSs and accuracy. Effect of variation in distance between the base stations on the localization accuracy is studied for achieving more compact Y- and L-shape configurations. When the distance between the BSs in the xy-plane is reduced to 1 and 0.50 m, accuracy reductions of around 0.5–1 and 1.5–2.5 cm were observed, respectively. This is because the configurations are more compact leading to lesser coverage area and also error due to trilateration.

The error obtained for mirror-based configuration [Fig. 5(b)] is in the range of about 2–3 cm for x- and y-axes and around 5 cm for z-axis. As mentioned in Section III, the BS4 is the mirror image of BS1, and its position is dependent on the x and y position of the mobile station. The mirror-based configuration gives more accurate results as four base stations are considered for localization, with one of the base stations not physically present, but supposed to be at a particular position reducing the effect of interference from obstacles. It is observed that x- and y-axis accuracy is much higher than the z-axis as the distance between BSs in z-direction is much less (0.5 m) than in x- or y-axis (1.5 m) due to experimental setting limitations. The average error in estimated azimuth and elevation angle when compared to the expected angles is 1° to 3° for all the configurations studied.

For the cuboid-shape configuration, the BSs occupy the four corners of the localization area. Hence, full volume of the localization space is utilized. In the case of the Y-shape and mirror-based configurations, the BS antennas occupy only half of the localization space (three corners), leading to 50% reduction in the space occupied. The L-shape configuration needs only 2-D plane (xz-plane) for placement of the BSs. Hence, the total localization space is free, and the 3-D localization accuracy obtained is comparable to other configurations studied.

Theoretical analysis has been performed through GDOP [13], which indicates the effectiveness of a geometric configuration. GDOP can be defined as

$$\mathrm{GDOP} = \sqrt{\mathrm{tr}(H^T H)^{-1}} \tag{6}$$

where

$$H = \begin{bmatrix} a_{x1} & a_{y1} & a_{z1} & 1 \\ a_{x2} & a_{y2} & a_{z2} & 1 \\ a_{x3} & a_{y3} & a_{z3} & 1 \\ a_{x4} & a_{y4} & a_{z4} & 1 \end{bmatrix}$$

and

$$a_{xi} = \frac{(x_i - x_m)}{r_i} \quad a_{yi} = \frac{(y_i - y_m)}{r_i} \quad a_{zi} = \frac{(z_i - z_m)}{r_i}.$$

The GDOP is computed for the different positions of the mobile station for each BS configuration in an area of $1.5 \times 1.5\ \mathrm{m}^2$. Horizontal Dilution of Precision (HDOP) and Vertical Dilution of Precision (VDOP) are also calculated for more detailed analysis. The average GDOP, HDOP, and VDOP values for cuboid-shape and mirror-based configurations are 2.6, 1.15, and 2.3, respectively. For Y- and L-shape configurations, the average values are 3.7, 1.6, and 3.22, respectively, which is in the range of DOP values (2–4) stating good accuracy [14].

VI. Conclusion

Experimental and analytical investigations are carried out using the proposed compact base-station configurations to achieve high accuracy within centimeter range. The difference in localization accuracy is theoretically analyzed using Geometric Dilution of Precision. All four configurations show significant accuracy improvements in the range of 2–3.5 cm for x-axis and y-axis and 3.5–5 cm for z-axis, which is a substantial gain over existing methods and commercial technologies. The mirror-based configuration demonstrated an advantage of having four BSs (three physical and one virtual), and hence higher accuracy can be obtained, which is similar to the commonly used cuboid-shape configuration. By confining the base stations into a smaller area such as the L-shape configuration, the compact setup and cost effectiveness provide a good compromise for the small degradation in detection accuracy. Next steps of the presented work will include implementation of the proposed configurations using UWB transceiver chipsets with the antenna integrated as one sensor unit in order to make the system more cost-effective and portable.

References

[1] S. Gezici and H. V. Poor, "Position estimation via ultra-wide-band signals," *Proc. IEEE*, vol. 97, no. 2, pp. 386–403, Feb. 2009.

[2] M. R. Mahfouz, C. Zhang, B. C. Merkl, M. J. Kuhn, and A. E. Fathy, "Investigation of high-accuracy indoor 3-D positioning using UWB technology," *IEEE Trans. Microw. Theory Tech.*, vol. 56, no. 6, pp. 1316–1330, Jun. 2008.

[3] Z. N. Low, J. H. Cheong, C. L. Law, W. T. Ng, and Y. J. Lee, "Pulse detection algorithm for line-of-sight (LOS) UWB ranging applications," *IEEE Antennas Wireless Propag. Lett.*, vol. 4, pp. 63–67, 2005.

[4] R. Zetik, J. Sachs, and R. Thoma, "UWB localization—Active and passive approach [ultra wideband radar]," in *Proc. 21st IEEE IMTC*, May 18–20, 2004, vol. 2, pp. 1005–1009.

[5] R. Ye and H. Liu, "UWB TDOA localization system: Receiver configuration analysis," in *Proc. ISSSE*, Sep. 17–20, 2010, vol. 1, pp. 1–4.

[6] R. Bharadwaj, A. Alomainy, and C. Parini, "Study of ultra wideband localisation techniques using various monitoring configurations," in *Proc. 6th EuCAP*, Mar. 26–30, 2012, pp. 2035–2038.

[7] A. Alomainy, A. Sani, A. Rahman, J. G. Santas, and H. Yang, "Transient characteristics of wearable antennas and radio propagation channels for ultrawideband body-centric wireless communications," *IEEE Trans. Antennas Propag.*, vol. 57, no. 4, pp. 875–884, Apr. 2009.

[8] Agilent Technologies, Santa Clara, CA, USA, "Agilent 2-port and 4-port PNA-X network analyzer," 2013 [Online]. Available: http://cp.literature.agilent.com/litweb/pdf/N5245-90008.pdf

[9] D. Dardari, A. Conti, U. Ferner, A. Giorgetti, and M. Z. Win, "Ranging with ultrawide bandwidth signals in multipath environments," *Proc. IEEE*, vol. 97, no. 2, pp. 404–426, Feb. 2009.

[10] A. H. Sayed, A. Tarighat, and N. Khajehnouri, "Network-based wireless location: Challenges faced in developing techniques for accurate wireless location information," *IEEE Signal Process. Mag.*, vol. 22, no. 4, pp. 24–40, Jul. 2005.

[11] I. Guvenc and Z. Sahinoglu, "Threshold-based TOA estimation for impulse radio UWB systems," in *Proc. IEEE ICU*, Sep. 5–8, 2005, pp. 420–425.

[12] D. Humphrey and M. Hedley, "Prior models for indoor super-resolution time of arrival estimation," in *Proc. 69th IEEE VTC-Spring*, Apr. 26–29, 2009, pp. 1–5.

[13] S. Zirari, P. Canalda, and F. Spies, "A very first geometric dilution of precision proposal for wireless access mobile networks," in *Proc. 1st SPACOMM*, Jul. 20–25, 2009, pp. 162–167.

[14] R. B. Langley, "Dilution of precision," *GPS World*, vol. 10, no. 5, pp. 52–59, May 1999.